MLSE and MAP Equalization for Transmission Over Doubly Selective Channels

Imad Barhumi, *Member, IEEE*, and Marc Moonen, *Fellow, IEEE*

***Abstract*—In this paper, equalization for transmission over doubly selective channels is discussed. The symbol-by-symbol maximum *a posteriori* probability (MAP) equalizer and the maximum-likelihood sequence estimation (MLSE) are discussed. The doubly selective channel is modeled using the basis expansion model (BEM). Using the BEM allows for an easy and low-complexity mechanism for constructing the channel trellis to implement the MLSE and the MAP equalizer. The MLSE and the MAP equalizer are implemented for single-carrier transmission and for multicarrier transmission implemented using orthogonal frequency-division multiplexing (OFDM). In this scenario, a complexity–diversity tradeoff can be observed. In addition, we propose a joint estimation and equalization technique for doubly selective channels. In this joint estimation and equalization technique, the channel state information (CSI) is obtained in an iterative manner. Simulation results show that the performance of the joint channel estimation and equalization approaches the performance when perfect CSI is available at the receiver.**

***Index Terms*—Channel estimation, doubly selective channels, maximum *a posteriori* equalizer, maximum-likelihood sequence estimation (MLSE), orthogonal frequency-division multiplexing (OFDM), single-carrier (SC) transmission.**

I. Introduction

THE WIRELESS communication channel is mainly characterized as a doubly selective channel, i.e., it is selective in both time and frequency. While multipath propagation gives rise to frequency selectivity, mobility and/or carrier frequency offset give rise to time selectivity. Frequency selectivity implies intersymbol interference (ISI), i.e., the transmitted signal is spread in time. On the other hand, time selectivity results in a spreading of the transmitted signal in the frequency domain or the so-called Doppler spread. Therefore, to provide reliable communication, advanced and efficient channel equalization and estimation techniques are necessary.

Equalizers, in general, can be classified according to their structure, i.e., as linear or nonlinear (e.g., decision feedback) equalizers. Equalizers can also be classified according to the optimization criterion used for the design. In particular, equalizers can be classified as zero forcing (ZF) when a solution that forces ISI to zero is sought, MMSE when the equalizer optimizes the mean-square error of the symbol estimate, or maximum likelihood when the maximum-likelihood sequence estimation (MLSE) criterion is utilized.

In the context of linear equalization of time-invariant (TI) channels, linear MMSE and ZF equalizers are investigated in [1]. Decision feedback equalizers (DFEs), where previously detected symbols are used to compensate for postcursor ISI, are discussed in [2]. The utilization of finite-impulse response (FIR) filters for DFEs is investigated in [3]. The MLSE for data transmission over TI channels with ISI is introduced in [4], where the MLSE is implemented using the Viterbi algorithm (VA).

For time-varying channels, linear MMSE and DFE equalizers using time-varying FIR filters are introduced in [5] and [6]. For orthogonal frequency-division multiplexing (OFDM) transmission over doubly selective channels, time-domain equalizers (TEQs) and frequency-domain per-tone equalizers (PTEQs) are introduced in [7]. For time-varying flat-fading channels, polynomial fitting of the one-tap time-varying channel is used to predict the channel, as proposed in [8]. Extending polynomial fitting over the whole packet (or using the sliding window approach) to time-varying frequency-selective channels is investigated in [9]. Adaptive MLSE is proposed in [10] to equalize time-varying channels. MLSE-based adaptive channel estimation and equalization are also proposed in [11]. However, this technique has difficulty tracking rapidly time-varying channels.

In this paper, we propose a symbol-by-symbol maximum *a posteriori* probability (MAP) equalizer and the MLSE for transmission over rapidly time-varying channels. The MAP equalizer is implemented using the Bahl–Cocke–Jelinek–Raviv (BCJR) algorithm [12], and the MLSE is implemented using the VA [13]. The time-varying channel is approximated using the basis expansion model (BEM). Using the BEM allows for an efficient low-complexity mechanism to update the branch metrics and therefore results in a more efficient implementation of the BCJR algorithm and VA. If it had not been for the true channel and basis expansion channel-model mismatch, the proposed equalizers would have been optimal. However, this optimality can be retained if the BEM channel has dimensionality equal to the block size or if the true channel exactly follows the BEM. The proposed equalizers are derived assuming that perfect channel state information (CSI) is available at the receiver. To facilitate a more realistic scenario, a joint channel estimation and equalization algorithm is proposed. An initial channel estimation is obtained based on pilot-symbol-assisted modulation (PSAM), and the equalized (estimated) symbols are then used to estimate the channel BEM coefficients. This joint

Manuscript received January 21, 2009; revised April 16, 2009, May 21, 2009, and May 23, 2009. First published June 10, 2009; current version published October 2, 2009. The review of this paper was coordinated by Dr. C. Cozzo.

I. Barhumi is with the Department of Electrical Engineering, United Arab Emirates University, Al-Ain 17555, United Arab Emirates (e-mail: imad.barhumi@uaeu.ac.ae).

M. Moonen is with the Department of Electrical Engineering, Katholieke Universiteit Leuven, 3001 Leuven, Belgium (e-mail: marc.moonen@esat.kuleuven.be).

Color versions of one or more of the figures in this paper are available online at http://ieeexplore.ieee.org.

Digital Object Identifier 10.1109/TVT.2009.2024537

0018-9545/$26.00 © 2009 IEEE

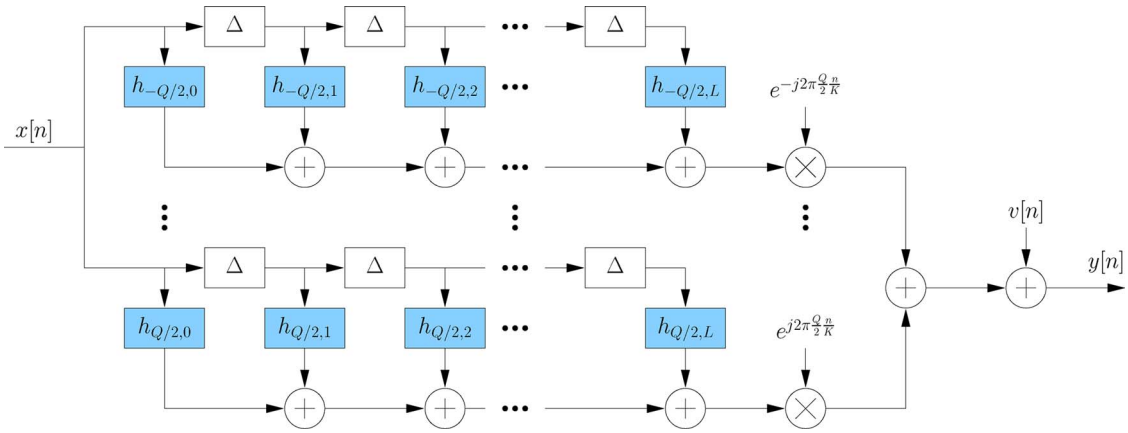


Fig. 1. Input–output relationship using the BEM.

channel estimation and equalization is repeated in an iterative manner. The proposed channel equalization and estimation techniques are applied to single-carrier (SC) and multicarrier (MC) transmission techniques. The MC transmission technique is implemented using OFDM.

This paper is organized as follows: The system model and the proposed equalizers are introduced in Section II. In Section III, we discuss the joint channel estimation and equalization algorithm. Our findings are confirmed by numerical simulations introduced in Section IV. Finally, our conclusions are drawn in Section V.

Notation: We use upper boldface letters and lower boldface letters to denote frequency- and time-domain vectors, respectively. Matrices are also denoted using boldface upper letters, where the difference with frequency-domain vectors should be clear from the context. Superscripts H, T, and $*$ denote the Hermitian transpose, transpose, and complex conjugate, respectively. We denote the $N \times N$ identity matrix as $\mathbf{I}_N$ and the $M \times N$ all-zero matrix as $\mathbf{0}_{M\times N}$. The N-dimensional unity vector with 1 at position $(N+k)_N + 1$ is denoted as $\mathbf{e}_k$, where $(a)_b$ denotes $a \bmod b$. Finally, $\mathrm{diag}\{\mathbf{x}\}$ denotes the diagonal matrix with vector $\mathbf{x}$ on the diagonal.

II. System Model

We consider transmission over a doubly selective single-input–single-output channel, where one transmit and one receive antenna are used. A data sequence $x[n]$ of length N is transmitted at a rate of $1/T$ symbol/s over the time-varying channel. The data sequence can be thought of as quadratic amplitude modulation (QAM) symbols for SC transmission or a time-domain equivalent of QAM frequency-domain symbols for MC transmission. The discrete-time baseband equivalent description of the received sequence at time index n is given by

$$y[n] = \sum_{l=0}^{L} g[n;l]x[n-l] + v[n] \tag{1}$$

where $g[n;\theta]$ is the discrete-time equivalent baseband representation of the time-varying frequency-selective channel, taking into account the physical multipath channel and the transmitter and receiver pulse-shaping filters. The channel order is given by $L = \lfloor \tau_{\max}/T \rfloor + 1$, with $\tau_{\max}$ being the channel maximum delay spread. Finally, $v[n]$ is the discrete-time additive white Gaussian noise (AWGN).

We use the BEM [14] to approximate the doubly selective channel $g[n;l]$, where the doubly selective channel is modeled as a time-varying FIR filter over a window of size N. For $n \in \{0,\ldots,N-1\}$, each tap of the time-varying FIR filter is expressed as a superposition of complex exponential basis functions with frequencies on a discrete Fourier transform (DFT) grid as[1]

$$h[n;l] = \sum_{q=-Q/2}^{Q/2} e^{j2\pi qn/K} h_{q,l} \tag{2}$$

where Q is the number of time-varying basis functions of the BEM satisfying $Q/(2KT) \geq f_{\max}$, with $f_{\max}$ being the channel maximum Doppler spread and $K \geq N$ being the BEM resolution. $h_{q,l}$ is the coefficient of the qth basis function of the lth tap, which is kept invariant for the transmission of a block of N symbols and may independently change from block to block.

Substituting (2) into (1), we obtain the following input–output relationship:

$$y[n] = \sum_{q=-Q/2}^{Q/2} \sum_{l=0}^{L} e^{j2\pi qn/K} h_{q,l} x[n-l] + v[n]. \tag{3}$$

The input–output relationship (3) is shown in Fig. 1.

Defining $\mathbf{y} = [y[0],\ldots,y[N-1]]^T$, in a block-level formulation, the received vector $\mathbf{y}$ can be written as

$$\mathbf{y} = \sum_{q=-Q/2}^{Q/2} \sum_{l=0}^{L} h_{q,l} \mathbf{D}_q \mathbf{Z}_l \mathbf{x} + \mathbf{v} \tag{4}$$

where $\mathbf{D}_q$ is a diagonal matrix with the qth basis function components on its diagonal $\mathbf{D}_q = \mathrm{diag}\{[1, e^{j2\pi q/K}, \ldots, e^{j2\pi q(N-1)/K}]^T\}$, and $\mathbf{Z}_l$ is an $N \times (N+L)$ Toeplitz matrix defined as $\mathbf{Z}_l = [\mathbf{0}_{N\times(L-l)}, \mathbf{I}_N, \mathbf{0}_{N\times l}]$. The transmitted

[1]Note that we use different notations for the true channel $g[n;l]$ and the BEM channel $h[n;l]$ to stress the fact that the BEM model is an approximation of the true channel. However, in the subsequent analysis, we proceed as if the channel follows the BEM exactly.

symbols vector $\mathbf{x}$ is defined as $\mathbf{x} = [x[-L], \ldots, x[N-1]]^T$, and finally, the additive noise vector $\mathbf{v}$ is similarly defined as $\mathbf{y}$.

A. MAP Equalization

In the following, the MAP equalizer is introduced for the case of SC transmission and OFDM transmission techniques.

1) SC Transmission: For SC transmission, the time-domain transmitted symbols $x[n]$ are drawn from a finite alphabet $\mathcal{X}$, i.e., $x[n] \in \mathcal{X}$. The MAP equalizer obtains an estimate of the transmitted symbol $x[n]$ at time index n that maximizes the *a posteriori* probability $\Pr(x[n] = x|\mathbf{y})$, i.e.,

$$\hat{x}[n] = \arg\max_{x \in \mathcal{X}} \Pr\left(x[n] = x|\mathbf{y}\right) \tag{5}$$

where x is drawn from the finite input alphabet $\mathcal{X}$ with cardinality $|\mathcal{X}| = M$. The MAP equalizer can be implemented based on the BCJR algorithm [12], where the forward recursion coefficient $\alpha_n(s)$ and backward coefficient $\beta_n(s)$ for state s at time index (which is sometimes referred to as recursion) n are obtained as

$$\alpha_n(s) = \sum_{\forall s' \in \mathcal{S}} \alpha_{n-1}(s')\gamma_{n-1}(s', s) \tag{6}$$

$$\beta_n(s) = \sum_{\forall s' \in \mathcal{S}} \beta_{n+1}(s')\gamma_n(s, s') \tag{7}$$

where $\mathcal{S}$ is the set of all possible states in the trellis describing the time-varying channel. The initial conditions for the forward recursion coefficients are $\alpha_{-1}(s_0) = 1$ and $\alpha_{-1}(s \neq s_0) = 0$, assuming that the initial state is known to be s_0. The initial conditions for the backward recursion coefficients are $\beta_N(s) = 1/|\mathcal{S}| \forall s \in \mathcal{S}$, assuming no trellis termination. If the trellis is terminated to some final state s^j, then the initial conditions for the backward recursion coefficients are $\beta_N(s^j) = 1$ and $\beta_N(s \neq s^j) = 0$. The term $\gamma_n(s', s)$ is the transition probability $\Pr(s_{n+1} = s', y[n]|s_n = s)$ from state s' to state s at time index n. Using Bayes' theorem, $\gamma_n(s', s)$ can be written as

$$\gamma_n(s', s) = \Pr(s_{n+1} = s'|s_n = s) \Pr\left(y[n]|s_n = s, s_{n+1} = s'\right). \tag{8}$$

The transition probability needs to be computed for every branch in the trellis describing the time-varying channel. To do so, we define $z^{(i,j)}[n]$ as the noiseless channel output symbol corresponding to the transition from state s^i to state s^j at time index n. In addition, define the sequence $\mathcal{X}^{(i,j)}$ as the length-$(L+1)$ sequence of symbols that characterizes the transition from state s^i to state s^j, i.e., $\mathcal{X}^{(i,j)} = \{x_0^{(i,j)}, \ldots, x_L^{(i,j)}\}$ for all possible combinations $i, j = 0, \ldots, M^L - 1$. The noiseless channel output $z^{(i,j)}[n]$ can then be written as

$$z^{(i,j)}[n] = \sum_{l=0}^{L} g[n; l] x_{L-l}^{(i,j)}. \tag{9}$$

Using the Euclidean distance, the channel branch metric for the transition from state s^i to state s^j at time index n is given by

$$r^{(i,j)}[n] = \left|y[n] - z^{(i,j)}[n]\right|^2. \tag{10}$$

Assuming AWGN with zero mean and variance σ_n^2, the transition probability from state s^i to state s^j at time index n $\gamma_n(s^i, s^j)$ can be obtained as

$$\gamma_n(s^i, s^j) = \begin{cases} \Pr\left(x[n] = x_L^{(i,j)}\right) \frac{\exp\left[-r^{(i,j)}/\left(2\sigma_n^2\right)\right]}{\sqrt{2\pi\sigma_n^2}}, & s^i \to s^j \\ 0, & \text{otherwise.} \end{cases} \tag{11}$$

For TI channels, the outputs $z^{(i,j)}[n]$ are also TI (independent of n), which means that, to run the BCJR algorithm, one state diagram or transition table containing $z^{(i,j)}[n]$ for all possible $\mathcal{X}^{(i,j)}$'s has to be constructed and used for the equalization process. For time-varying channels, the output symbols $z^{(i,j)}[n]$ are also time varying as they depend on the CSI at every time instant n. Therefore, to run the BCJR algorithm, the transition table has to be recomputed for each recursion. A more efficient procedure can be obtained by exploiting the BEM, as explained in the following.

Using the BEM to approximate the doubly selective channel, we can write the noiseless channel output $z^{(i,j)}[n]$ in (9) as

$$\begin{aligned} z^{(i,j)}[n] &= \sum_{-Q/2}^{Q/2} \left(\sum_{l=0}^{L} h_{q,l} x_{L-l}^{(i,j)}\right) e^{j2\pi qn/K} \\ &= \sum_{q=-Q/2}^{Q/2} z_q^{(i,j)} e^{j2\pi qn/K}. \end{aligned} \tag{12}$$

Therefore, the branch metric for the transition from state s^i to state s^j at time index n can be written as

$$r^{(i,j)}[n] = \left|y[n] - \sum_{q=-Q/2}^{Q/2} z_q^{(i,j)} e^{j2\pi qnK}\right|^2. \tag{13}$$

Using the BEM as shown in (12) to implement the BCJR algorithm, $(Q+1)$ TI transition tables have to be constructed. Each transition table corresponds to a branch in the BEM channel. The transition table corresponding to the qth branch contains the elements $z_q^{(i,j)}$ for all possible $\mathcal{X}^{(i,j)}$'s. Hence, the complexity of computing/updating $z^{(i,j)}[n]$ in (12) is $(Q+1)M^L$ multiply–add (MA) operations, compared with $(L+1)M^L$ MA operations if (9) is used. However, the latter requires the CSI at every time instant, whereas (12) requires only the knowledge of the channel BEM coefficients. The computational complexity is very much reduced for the case $Q \ll L$, which is the case for most high-data-rate wireless communication channels.

2) OFDM Transmission: For OFDM transmission, the information-bearing symbols are parsed into blocks of N frequency-domain QAM symbols. Each block is then transformed to the time domain by inverse DFT. A cyclic prefix (CP) of length $\nu \geq L$ is added to the head of each block. The time-domain blocks are then serially transmitted over the time-varying channel. Assuming that S_k is the transmitted symbol on the kth subcarrier of the OFDM block, $x[n]$ can be written as

$$x[n] = \frac{1}{\sqrt{N}} \sum_{k=0}^{N-1} S_k e^{j2\pi(n-\nu)k/N}, \qquad n = 0, \ldots, N+\nu-1.$$

Note that this description includes the transmission of a CP of length ν. The received sequence after removing the CP can be written as

$$\mathbf{y} = \sum_{q=-Q/2}^{Q/2} \sum_{l=0}^{L} h_{q,l} \mathbf{D}_q \bar{\mathbf{Z}}_l \mathbf{F}^H \mathbf{S} + \mathbf{v} \tag{14}$$

where $\mathbf{F}$ is an $N \times N$ unitary DFT matrix; $\bar{\mathbf{Z}}_l$ is an $N \times N$ circular matrix, with $\mathbf{e}_l$ as its first column; and $\mathbf{S}$ is the frequency-domain transmitted vector $\mathbf{S} = [S_0, \ldots, S_{N-1}]^T$. The frequency-domain symbols S_k's are drawn from the finite input alphabet[2] $\mathcal{X}$, i.e., $S_k \in \mathcal{X}$. Define $\mathbf{Y} = [Y_0, \ldots, Y_{N-1}]^T$ as the received vector in the frequency domain; then, $\mathbf{Y}$ can be written as

$$\mathbf{Y} = \sum_{q=-Q/2}^{Q/2} \sum_{l=0}^{L} h_{q,l} \mathbf{F} \mathbf{D}_q \bar{\mathbf{Z}}_l \mathbf{F}^H \mathbf{S} + \mathbf{V} \tag{15}$$

where $\mathbf{V} = [V_0, \ldots, V_{N-1}]^T$ is the noise vector in the frequency domain, with V_k being the noise on the kth subcarrier.

For $K = N$, i.e., when the BEM basis functions are taken on a DFT grid of size N, we can use the properties $\mathbf{D}_q = \mathbf{F}^H \bar{\mathbf{Z}}_q \mathbf{F}$ and $\bar{\mathbf{Z}}_l = \mathbf{F}^H \mathbf{D}_{-l} \mathbf{F}$. Hence, (15) can be written as

$$\mathbf{Y} = \sum_{q=-Q/2}^{Q/2} \sum_{l=0}^{L} h_{q,l} \bar{\mathbf{Z}}_q \mathbf{D}_{-l} \mathbf{S} + \mathbf{V}. \tag{16}$$

Using the property $\bar{\mathbf{Z}}_q \mathbf{D}_{-l} = e^{j2\pi ql/N} \mathbf{D}_{-l} \bar{\mathbf{Z}}_q$, we obtain

$$\mathbf{Y} = \sum_{l=0}^{L} \sum_{q=-Q/2}^{Q/2} \tilde{h}_{q,l} \mathbf{D}_{-l} \bar{\mathbf{Z}}_q \mathbf{S} + \mathbf{V} \tag{17}$$

where $\tilde{h}_{q,l} = e^{j2\pi ql/N} h_{q,l}$. Hence, the input–output relationship on the kth subcarrier can be written as

$$Y_k = \sum_{l=0}^{L} \sum_{q=-Q/2}^{Q/2} e^{-j2\pi kl/N} \tilde{h}_{q,l} S_{(k-q)_N} + V_k. \tag{18}$$

Note the similarity between (18) and (3). From (18), it is observed that, when using a BEM resolution $K = N$, OFDM transmission corresponds to SC transmission, where the doubly selective channel is now of order Q, instead of L, for SC transmission, and the time variation is captured by means of $(L+1)$, instead of $(Q+1)$, time-varying complex exponential basis functions for SC transmission. The channel BEM coefficients are now characterized by $\tilde{h}_{q,l}$. However, due to the CP, the linear convolution in SC transmission is now replaced by a cyclic convolution. Hence, we can depict a figure similar to Fig. 1 but with input S_k and output Y_k to describe the input–output relationship in (18). Therefore, the MLSE and the MAP equalizer for OFDM transmission are obtained in a similar fashion as that for SC transmission. The branch metrics of the trellis are obtained as follows: Define $\mathcal{S}^{(i,j)}$ as the length-$(Q+1)$ sequence of symbols that characterizes the transition from state s^i to state s^j, i.e., $\mathcal{S}^{(i,j)} = \{S_0^{(i,j)}, \ldots, S_Q^{(i,j)}\}$ for all possible combinations $i, j = 0, \ldots, M^Q - 1$. The noiseless channel output symbol $Z^{(i,j)}[k]$ of the transition from state s^i to state s^j at recursion k, for a given subcarrier index k, can be written as

$$Z^{(i,j)}[k] = \sum_{l=0}^{L} Z_l^{(i,j)} e^{-j2\pi lk/N} \tag{19}$$

where $Z_l^{(i,j)}$ is given by

$$Z_l^{(i,j)} = \sum_{q=-Q/2}^{Q/2} \tilde{h}_{q,l} S_{Q/2-q}^{(i,j)}. \tag{20}$$

Using the Euclidean distance, the branch metric for the transition from state s^i to state s^j at recursion k is given by

$$R^{(i,j)}[k] = \left| y_k - Z^{(i,j)}[k] \right|^2. \tag{21}$$

The MAP equalization is then performed in the same manner as in the case of SC transmission using the BCJR algorithm. The BCJR algorithm is then implemented in the frequency domain, with the transition probability $\gamma_k(s^i, s^j)$ defined as

$$\gamma_k(s^i, s^j) = \Pr(s_{k+1} = s^i | s_k = s^j) \Pr(Y_k | s_k = s^j, s_{k+1} = s^i) \tag{22}$$

which can be computed as in (11) by replacing $y[n]$ with Y_k, $r^{(i,j)}[n]$ with $R^{(i,j)}[k]$, and $\mathcal{X}^{(i,j)}$ with $\mathcal{S}^{(i,j)}$.

For a BEM resolution $K > N$, inter-carrier interference (ICI) is not limited and covers the whole OFDM block, which prevents the development of a practical MLSE or MAP equalizer using the trellis-based BCJR algorithm. However, the main part of the ICI typically comes from the neighboring Q subcarriers, and therefore, the preceding model and analysis may be used as a good approximation.

B. MLSE

For channels with memory where ISI occurs, the MLSE searches for the sequence $\mathcal{X}^{(j')}$ that maximizes the conditional probability $\Pr(\mathbf{y}|\mathcal{X}^{(j)})$, i.e.,

$$\mathcal{X}^{(j')} = \max_j \Pr\left(\mathbf{y}|\mathcal{X}^{(j)}\right) \tag{23}$$

where the sequence $\mathcal{X}^{(j)} = \{x_0^{(j)}, \ldots, x_{N-1}^{(j)}\}$, with $x_i^{(j)} \in \mathcal{X}$. The sequence that maximizes the conditional probability can be obtained by performing an exhaustive search over the M^N different sequences. For a large block size and/or large alphabet size, this exhaustive search may be prohibitive for practical applications. For ISI channels with finite memory of length L, which can be described as a finite-state machine, the VA can be invoked to find the most likely state transition sequence in the state diagram (or the trellis). Details on the VA can be found in [4].

[2]Note that we choose to define the frequency-domain input alphabet to be the same as the time-domain input alphabet for SC transmission $\mathcal{X}$.

The number of states in the state diagram or the trellis in this case is M^L, where, usually, $L \ll N$.

After computing the branch metrics as in (13) for SC transmission and as in (21) for OFDM transmission, the add–compare–select (ACS) step of the VA is performed. For SC transmission, we define $m^{(j)}[n]$ as the path metric of state s^j at time index n and set $\mathcal{I}^{(j)}$ as the set of states that have transitions to state s^j. The branch metric of state s^j at time index n is then given as

$$m^{(j)}[n] = \min_{i \in \mathcal{I}^{(j)}} \left(m^{(i)}[n-1] + r^{(i,j)}[n] \right).$$

The branch i that satisfies the preceding equation represents the most likely path leading into state s^j at recursion n.

For OFDM transmission, the ACS operation of the VA is performed as follows: Define $M^{(j)}[k]$ as the path metric of state s^j at subcarrier k and $\mathcal{I}^{(j)}$ as the set of all states that have transitions to state s^j. The path metric of state s^j at subcarrier k is then given as

$$M^{(j)}[k] = \min_{i \in \mathcal{I}^{(j)}} \left(M^{(i)}[k-1] + R^{(i,j)}[k] \right).$$

In conclusion, as in the case of the MAP equalizer, instead of recomputing the trellis outputs for each time instant, taking into account the channel status at that time instant, the BEM allows for an easy and computationally efficient mechanism to run the VA for time-varying channels. In this sense, $(Q+1)$ TI transition tables are precomputed and stored, and at each time instant, the branch metrics are updated using (12). Note that, in most cases, Q is a small number, e.g., $Q = 2$ and 4.

C. Complexity Diversity Tradeoff

For a block of N symbols, running the MLSE and/or the MAP equalizer in the time domain (SC transmission) and using perfect CSI requires $\mathcal{O}(N(L+1)M^L)$ MA operations. It also requires M^L memory locations to store the transition tables, which are to be recomputed for each time instant. Running the proposed algorithms in the time domain and using the BEM requires $\mathcal{O}(N(Q+1)M^L)$ MA operations, in addition to $(Q+1)M^L$ memory locations to store the $(Q+1)$ transition tables that characterize the state diagrams. Note that these tables are computed once for every block of N symbols.

Running the MLSE and/or the MAP equalizer in the frequency domain (OFDM) and using the BEM requires $\mathcal{O}(N(Q+1)M^Q)$ MA operations, in addition to $(L+1)M^Q$ memory locations to store the $(L+1)$ transition tables that characterize the state diagrams.

In the time domain, the MLSE and/or the MAP equalizer are capable of exploiting the multipath diversity, where the multipath diversity is of the order $L+1$, whereas in the frequency domain, they are capable of exploiting the Doppler diversity. Using the BEM, the diversity order is equal to $Q+1$. In this sense, we can trade off diversity and complexity. On the one hand, for $L > Q$, running the MLSE and/or the MAP equalizer in the frequency domain is less complex than running them in the time domain for a fairly small alphabet size and large block size. However, this comes at the cost of less diversity. Similarly, for $Q > L$, running these techniques in the time domain is less complex but again comes at the cost of less diversity. Exploiting the full, multipath, and Doppler diversity is possible by using maximum diversity techniques in conjunction with the MLSE and/or the MAP equalizer [15].



Fig. 2. Optimal training for doubly selective channels.

III. Joint Channel Estimation and Equalization

In our analysis so far, the CSI is assumed to be perfectly known at the receiver to accomplish the equalization process. In practice, the CSI needs to be estimated at the receiver, which will be subject to estimation errors and, hence, will influence the performance of the equalizers. In this section, we discuss joint channel estimation and equalization [16], where the initial estimate of the channel BEM coefficients is obtained using the PSAM technique, as proposed in [17]. The PSAM-based channel estimate is then used to construct the transition tables that are necessary to run the MLSE or the MAP equalizer. The equalizer output (estimated data symbols) is then used to reestimate the BEM coefficients of the time-varying channel. This process of joint channel estimation and equalization is repeated until either the maximum number of iterations is reached or any other stopping criterion is satisfied.

A. SC PSAM

For SC, the multiplexing of the data/training symbol is shown in Fig. 2, where the training part consists of a training symbol surrounded by L zeros on each side. Assuming that P such training clusters are used and the pilot symbols are located at positions $n_0, \ldots, n_{P-1}$, the input–output relation on the pilot positions can be written as

$$\mathbf{y}_{t,l} = \mathbf{X}_t \mathbf{g}_{t,l} + \mathbf{v}_{t,l} \tag{24}$$

where subscript t refers to training. The received vector corresponding to training $\mathbf{y}_{t,l}$ is defined as $\mathbf{y}_{t,l} = [y[n_0 + l], \ldots, y[n_{P-1} + l]]^T$, $\mathbf{X}_t = \mathrm{diag}\{[x[n_0], \ldots, x[n_{P-1}]]^T\}$, and $\mathbf{g}_{t,l} = [g[n_0; l], \ldots, g[n_{P-1}; l]]^T$, and $\mathbf{v}_{t,l}$ is similarly defined as $\mathbf{y}_{t,l}$, $\mathbf{v}_{t,l} = [v[n_0 + l], \ldots, v[n_{P-1} + l]]^T$.

The BEM channel coefficients are obtained by a least-squares (LS) fitting of the exact channel. However, since the exact channel is unknown, first, an estimate of this channel has to be acquired. From (24), an estimate of the lth tap of the time-varying channel $\hat{\mathbf{g}}_l = [\hat{g}[0; l], \ldots, \hat{g}[N-1; l]]^T$ is obtained by applying a $P \times N$ interpolation matrix $\mathbf{W}_l$ as

$$\hat{\mathbf{g}}_l = \mathbf{W}_l^H \mathbf{y}_{t,l}. \tag{25}$$

The optimal MMSE interpolation matrix is then found as

$$\mathbf{W}_{\mathrm{MMSE},l} = \left(\mathbf{X}_t \mathbf{R}_{p,l} \mathbf{X}_t^* + \mathbf{R}_{\tilde{v}} \right)^{-1} \mathbf{X}_t \mathbf{R}_{g,l} \tag{26}$$

where $\mathbf{R}_{p,l}$ is the lth tap channel correlation matrix on the pilots given by

$$\mathbf{R}_{p,l} = \begin{bmatrix} r_{g,l}[0] & \cdots & r_{g,l}[n_0 - n_{P-1}] \\ r_{g,l}[n_1 - n_0] & \cdots & r_{g,l}[n_1 - n_{P-1}] \\ \vdots & \ddots & \vdots \\ r_{g,l}[n_{P-1} - n_0] & \cdots & r_{g,l}[0] \end{bmatrix} \quad (27)$$

and $\mathbf{R}_{g,l}$ is given by

$$\mathbf{R}_{g,l} = \begin{bmatrix} r_{g,l}[n_0] & \cdots & r_{g,l}[n_0 - N + 1] \\ r_{g,l}[n_1] & \cdots & r_{g,l}[n_1 - N + 1] \\ \vdots & \ddots & \vdots \\ r_{g,l}[n_{P-1}] & \cdots & r_{g,l}[n_{P-1} - N + 1] \end{bmatrix} \quad (28)$$

where $r_{g,l}[k] = \mathcal{E}\{g[n;l]g^*[n-k;l]\}$. $\mathbf{R}_{\tilde{v}}$ is the covariance matrix of the channel estimation error at the pilot positions. Both $\mathbf{R}_{p,l}$ and $\mathbf{R}_{g,l}$ are assumed to be known. Assuming Jakes' model, then only knowledge of the system maximum Doppler shift $f_{\max}$ and the power delay profile are required. Note that, for channels with uniform power delay profile, matrices $\mathbf{R}_{p,l}$, $\mathbf{R}_{g,l}$, and $\mathbf{W}_{\mathrm{MMSE},l}$ are identical and independent of l, which means that they have to be computed only once.

An estimate of the BEM coefficients of the lth tap $\mathbf{h}_l = [h_{-Q/2,l}, \ldots, h_{Q/2,l}]^T$ is then obtained by LS fitting the estimated channel to its BEM model as

$$\begin{aligned} \hat{\mathbf{h}}_l &= \boldsymbol{\mathcal{L}}^{\dagger} \hat{\mathbf{g}}_l \\ &= \boldsymbol{\mathcal{L}}^{\dagger} \mathbf{W}_{\mathrm{MMSE},l}^H \mathbf{y}_{t,l} \end{aligned} \quad (29)$$

where $\mathcal{L}$ is defined as

$$\mathcal{L} = \begin{bmatrix} 1 & \cdots & 1 \\ e^{-j2\pi \frac{Q}{2} \frac{1}{K}} & \cdots & e^{j2\pi \frac{Q}{2} \frac{1}{K}} \\ \vdots & & \vdots \\ e^{-j2\pi \frac{Q}{2} \frac{N-1}{K}} & \cdots & e^{j2\pi \frac{Q}{2} \frac{N-1}{K}} \end{bmatrix}. \quad (30)$$

This initial estimate of the channel BEM coefficients is then used to build the transition tables necessary to implement the proposed equalizers. The estimated data symbol obtained for the MLSE and/or the MAP equalizer are then used to reestimate the BEM coefficients of the time-varying channel. Note that, for the MAP equalizer, soft or hard outputs may be used to estimate the channel. For the VA in its current form, only hard outputs are utilized for channel estimation. However, soft-output VA [18] can be used to obtain soft outputs. Simulation results show that joint schemes that utilize hard equalizer outputs for channel estimation outperform those that utilize soft equalizer outputs.

Starting from the input–output relationship (4), the received vector $\mathbf{y}$ can be written as

$$\mathbf{y} = \sum_{q=-Q/2}^{q/2} \mathbf{D}_q \mathbf{X} \mathbf{h}_q + \mathbf{v} \quad (31)$$

where $\mathbf{X}$ is an $N \times (L+1)$ Toeplitz matrix with first row $[x[0], \ldots, x[-L]]$ and first column $[x[0], \ldots, x[N-1]]^T$, and $\mathbf{h}_q = [h_{q,0}, \ldots, h_{q,L}]^T$. Defining $\boldsymbol{\mathcal{X}} = [\mathbf{X}_{-Q/2}, \ldots, \mathbf{X}_{Q/2}]$, with $\mathbf{X}_q = \mathbf{D}_q \mathbf{X}$, and $\mathbf{h} = [\mathbf{h}_{-Q/2}^T, \ldots, \mathbf{h}_{Q/2}^T]^T$, the input–output relationship can finally be written as

$$\mathbf{y} = \boldsymbol{\mathcal{X}} \mathbf{h} + \mathbf{v}. \quad (32)$$

The exact data symbols are unknown at the receiver, but an estimate of these data symbols $\hat{\boldsymbol{\mathcal{X}}}$ is obtained from the MLSE and/or the MAP equalizer. Hence, an estimate of the BEM coefficients of the time-varying channel can be obtained using LS as

$$\hat{\mathbf{h}} = \left(\hat{\boldsymbol{\mathcal{X}}}^H \mathbf{R}_v^{-1} \hat{\boldsymbol{\mathcal{X}}} \right)^{-1} \hat{\boldsymbol{\mathcal{X}}}^H \mathbf{R}_v^{-1} \mathbf{y} \quad (33)$$

or using the MMSE criterion as

$$\hat{\mathbf{h}} = \hat{\boldsymbol{\mathcal{X}}}^H \left(\hat{\boldsymbol{\mathcal{X}}} \hat{\boldsymbol{\mathcal{X}}}^H + \mathbf{R}_v \right)^{-1} \mathbf{y} \quad (34)$$

where the channel BEM coefficients are assumed to be zero-mean independent identically distributed (i.i.d.) complex Gaussian random variables with variance $\sigma_h^2 = 1/2(Q+1)$ per dimension.

For white noise, the channel estimate becomes

$$\hat{\mathbf{h}} = \left(\hat{\boldsymbol{\mathcal{X}}}^H \hat{\boldsymbol{\mathcal{X}}} \right)^{-1} \hat{\boldsymbol{\mathcal{X}}}^H \mathbf{y} \quad (35)$$

for the LS case and

$$\hat{\mathbf{h}} = \left(\hat{\boldsymbol{\mathcal{X}}}^H \hat{\boldsymbol{\mathcal{X}}} + \sigma_n^2 \mathbf{I}_{(Q+1)(L+1)} \right)^{-1} \hat{\boldsymbol{\mathcal{X}}}^H \mathbf{y} \quad (36)$$

for the MMSE case.

The estimate of the BEM coefficients of the time-varying channel obtained in (33) or (34) is then used to rerun the MLSE and/or the MAP equalizer. This requires the time-varying channel transition tables to be recomputed according to the new channel estimates. This process of joint channel estimation and equalization is performed in an iterative manner. The iterations are performed until the maximum number of iterations is reached or until convergence. Note that, if no pilot symbols are available, the joint channel estimation and equalization can be performed in a blind fashion, where the BEM coefficients of the channel are randomly initialized [19]. In this case, there is no guarantee that the BEM coefficients will converge to a global solution. However, with the utilization of PSAM, the convergence to a global solution can be guaranteed with a probability of 1.

B. OFDM PSAM

For OFDM, data and training multiplexing are similar to those shown in Fig. 2, except that the pilot symbols are surrounded with Q zeros from each side, instead of L zeros, for SC transmission. Channel estimation can then be performed in a similar fashion but in the frequency domain.

Starting from (17), the received vector $\mathbf{Y}$ can be written as

$$\mathbf{Y} = \boldsymbol{\mathcal{S}} \tilde{\mathbf{h}} + \mathbf{V} \quad (37)$$

where $\tilde{\mathbf{h}} = [\tilde{\mathbf{h}}_0, \ldots, \tilde{\mathbf{h}}_L^T]^T$ (with $\tilde{\mathbf{h}}_l = [\tilde{h}_{-Q/2,l}, \ldots, \tilde{h}_{Q/2,l}]^T$), and $\boldsymbol{\mathcal{S}} = [\boldsymbol{\mathcal{S}}_0, \ldots, \boldsymbol{\mathcal{S}}_L]$ (with $\boldsymbol{\mathcal{S}}_l = \mathbf{D}_{-l} \mathbf{S}_{\mathrm{circ}}$, where $\mathbf{S}_{\mathrm{circ}}$

is an $N \times (Q+1)$ circulant matrix with first column $[S_{N-Q/2}, \ldots, S_{N-1}, S_0, \ldots, S_{N-Q/2-1}]^T$). Hence, an estimate of the BEM coefficients can be obtained similar to (33) for the LS case and similar to (34) for the MMSE case by replacing $\hat{\boldsymbol{\mathcal{X}}}$ with an estimate of the frequency-domain symbols $\hat{\boldsymbol{\mathcal{S}}}$ obtained by the MLSE and/or the MAP equalizer.

IV. Numerical Results

In this section, we present simulation results for the proposed equalization techniques for SC and OFDM transmissions over doubly selective channels. In these simulations, uncoded quadrature phase-shift keying modulation is used. In the first scenario, the channel is assumed to be perfectly known at the receiver. In the second scenario, the performance of the proposed equalizers is evaluated when combined with channel estimation.

A. Perfect CSI

In this section, we assume that perfect CSI is available at the receiver. With perfect CSI, we mean that the coefficients of the BEM model are obtained by an LS fitting of the exact doubly selective channel in the noiseless case.

1) SC Transmission: For SC transmission, the doubly selective channel is assumed to be of the order $L = 3$. The channel taps are simulated as i.i.d. random variables correlated in time according to Jakes' model with correlation function $r_h[n] = J_0(2\pi n f_{\max} T)$, where J_0 is the zeroth-order Bessel function of the first kind, and $f_{\max} T = 0.001$ is the maximum normalized Doppler spread. A window of size $N = 800$ is considered in the simulations. Two BEM resolutions are considered, i.e., $K = N$ and $K = 2N$. For $K = N$, the number of basis functions is then obtained as $Q = 2$, whereas for $K = 2N$, the number of basis functions is obtained as $Q = 4$. Alongside the MLSE and the MAP equalizer, the linear MMSE equalizer and the DFE are examined. The feedforward and feedback filters are implemented as time-varying FIR filters designed according to the BEM [5], [6]. The feedforward filter is designed to be of the order $L' = 20$, and the number of basis functions is $Q' = 20$; the feedback filter is designed to be on the order $L'' = 3$, and the number of basis functions is $Q'' = 4$. Note that the complexity of the MLSE and the MAP equalizer is linear in Q and exponential in L, whereas it is cubic in $(Q + Q' + 1)(L + L' + 1)$ for the linear MMSE equalizer and the DFE. The performance is measured in terms of the bit error rate (BER) versus signal-to-noise ratio (SNR). The SNR is defined as $(L+1)E_s/\sigma_n^2$, where E_s is the transmitted symbol energy, and σ_n^2 is the AWGN variance. The simulation results are shown in Fig. 3. In all cases, the MLSE and the MAP equalizer exhibit the same BER performance, which is expected for uncoded transmission. For $K = N$, the MLSE, the MAP equalizer, the linear MMSE, and the DFE all suffer from an early error floor at about BER $= 3 \times 10^{-2}$. The MLSE and the MAP equalizer slightly outperform the linear MMSE equalizer and the DFE but not significantly so. For $K = 2N$, the MAP equalizer and the MLSE significantly outperform the linear MMSE equalizer and the DFE. An SNR gain of 4 dB is observed for the MLSE and the MAP equalizer over the linear MMSE equalizer, whereas an SNR gain of 2 dB is observed over the DFE. The performance of the MLSE over TI channels is simulated, with the channel order being $L = 3$. As can clearly be seen from the figure, the performance of the MAP equalizer or the MLSE for time-varying channels coincides with the performance of the MLSE for TI channels. This confirms the fact that the MLSE and the MAP equalizer in the time domain are capable of exploiting the multipath diversity. The matched filter bound (MFB) [20] for TI channels is also included in the plot. An SNR loss of about 1 dB is observed for the MLSE and the MAP equalizer, compared with the MFB. Clearly, the BER slope of the MLSE is the same as that of the MFB, which again confirms that the MLSE and the MAP equalizer are capable of exploiting the multipath diversity.

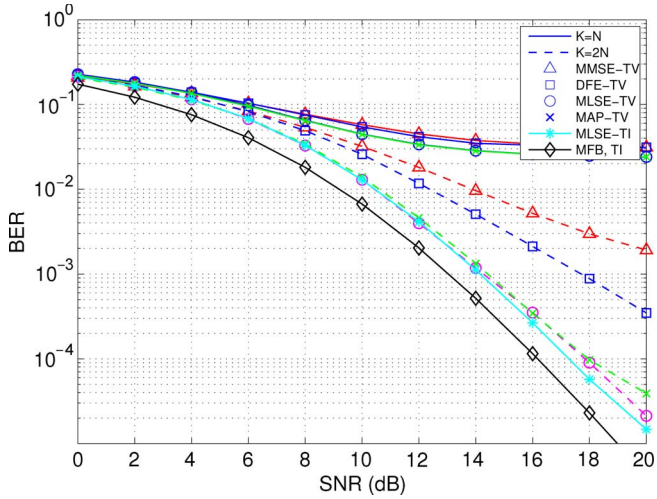


Fig. 3. Perfect CSI equalization for SC transmission.

2) OFDM Transmission: For OFDM transmission, we consider a doubly selective channel that is modeled using the BEM with order $L = 6$ and the number of basis functions $Q = 2$. The BEM coefficients are simulated as complex Gaussian random variables with zero mean and unit variance. The SNR is then defined as SNR $= (Q+1)(L+1)E_s/\sigma_n^2$. Alongside the MLSE and the MAP equalizer, the time-varying MMSE PTEQ is also examined [7]. For the PTEQ, the number of basis functions $Q' = 8$ and the number of basis functions $Q' = 14$ are considered. The simulation results corresponding to this setup are shown in Fig. 4. Both the MLSE and the MAP equalizer exhibit the same performance. Compared with the MMSE PTEQ, the MAP equalizer and MLSE significantly outperform the MMSE PTEQ for both cases $Q' = 8$ and $Q' = 14$. The SNR gain is 4.2 dB over the MMSE PTEQ with $Q' = 8$, whereas it is 3.2 dB over the MMSE PTEQ with $Q' = 14$. Again, an SNR loss of less than 1 dB is observed for the MAP equalizer and MLSE, compared with the MFB of the time-varying channels. In this case, the MFB is equivalent to the MFB of a TI channel with order equal to the number of basis functions $Q = 2$. Hence, a maximum diversity of order 3 can be achieved. The BER slope of the MLSE or the MAP equalizer is clearly the same as that of the MFB for time-varying channels, which confirms the fact that these equalizers in the frequency domain are capable of exploiting the Doppler diversity. The

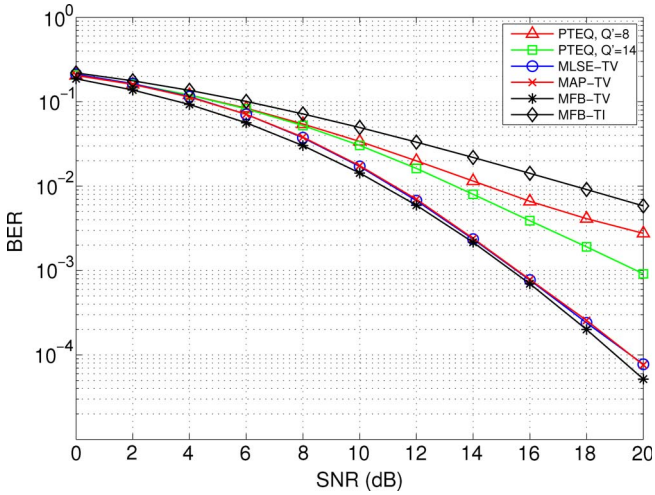


Fig. 4. Perfect CSI equalization for OFDM transmission.

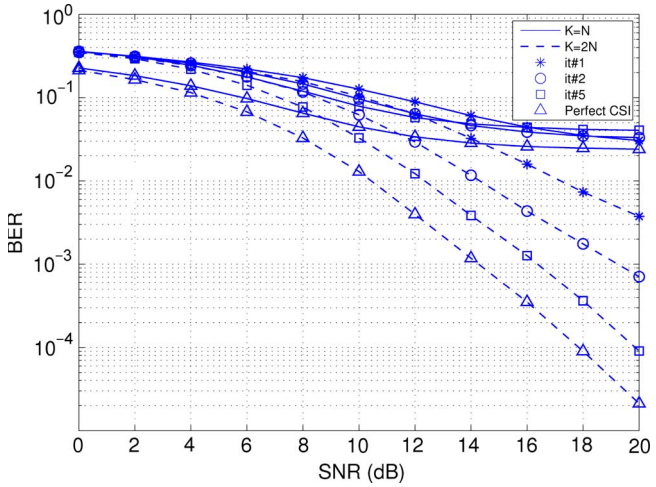


Fig. 5. Joint MAP and MLSE channel estimation and equalization for SC transmission.

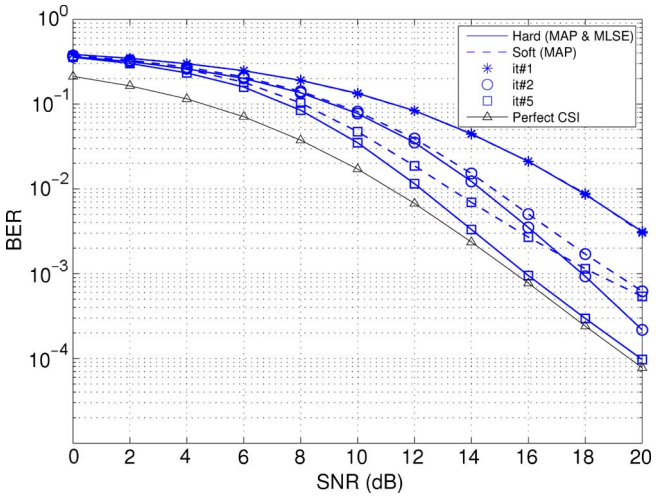


Fig. 6. Joint MAP and MLSE channel estimation and equalization for OFDM transmission.

MFB for OFDM transmission over TI channels is also plotted; the diversity order in this case is equal to unity.

B. Joint Channel Estimation and Equalization

In this section, the channel is assumed to be unknown at the receiver side. The PSAM technique is used to obtain an initial estimate of the BEM coefficients of the channel. A joint channel estimation and equalization is then performed in an iterative manner. The MLSE and the MAP equalizer are used. The MLSE provides hard outputs (hard VA is assumed), whereas the MAP equalizer provides hard and soft outputs. For the MAP equalizer, the hard and/or soft outputs are used for channel estimation.

1) SC Transmission: An initial channel estimate is obtained using the PSAM technique. The pilot symbols are designed to be equipowered and equispaced. With D, which is the spacing between the pilot symbols, the number of pilot symbols is computed as $P = \lfloor N/D \rfloor + 1$. Since we have $Q + 1 = 5$, which is suitable for the BEM resolution $K = 2N$, the spacing between the pilot symbols is chosen as $D = 165$, which corresponds to $P = 5$ pilot symbols dedicated for training. Each pilot symbol is surrounded by L zeros on each side. Therefore, the training overhead is $(2L + 1)P/N = 4.4\%$. In the simulations, five iterations are performed. As shown in Fig. 5, for $K = N$, all BER curves suffer from an early error floor that increases by the number of iterations. This is due to the fact that, for $K = N$, the modeling error is quite high, which leads to a propagation of error as the number of iterations increases. For $K = 2N$, the SNR gain for iteration 2 over the first iteration is about 3.9 dB, and that for iteration 5 over iteration 2 is about 2 dB. For iteration 5, the SNR loss is about 2 dB, compared with the case of perfect CSI, where SNR loss figures are computed at BER $= 10^{-2}$. The same performance is observed for the MLSE and the MAP equalizer for soft- and hard-output channel estimations.

2) OFDM Transmission: PSAM is used to obtain an initial estimate of the channel. The training symbols are designed to be equipowered and equispaced in frequency. The training symbols are of Kronecker delta type. The training scheme consists of $(L + 1)$ training clusters, where, in each cluster, a pilot symbol is surrounded by Q zeros on each side. The training overhead is then computed as $(L + 1)(2Q + 1)/N = 6.8\%$. As shown in Fig. 6, the SNR gain of iteration 2 over the first iteration is 2.9 dB for the MLSE and the MAP equalizer with either soft- or hard-output estimates. The SNR gain of iteration 5 is 0.9 dB for the MAP equalizer with soft-output estimates, whereas it is 2.1 dB for the MLSE and the MAP equalizer with hard-output estimates, all of which are computed at BER $= 10^{-2}$. For iteration 5, the BER curve approaches the performance when perfect CSI is available at the receiver, and the SNR loss is less than 0.5 dB at BER $\geq 10^{-3}$.

V. Conclusion

In this paper, the MLSE and the MAP equalizer for transmission over doubly selective channels have been proposed. The MAP equalizer has been implemented using the BCJR algorithm, and the MLSE has been implemented using the VA. SC transmission and MC transmission implemented using OFDM have been considered. The BEM has been used to

approximate the doubly selective channel. Using the BEM, the doubly selective channel can be viewed as a bank of TI FIR filters, where the time variation of each filter is captured by means of a time-varying complex exponential basis function. By doing so, we have shown that the branch metrics required for the MAP equalizer and the MLSE can be computed and updated in a similar fashion as the BEM. This, however, comes at the cost of extra memory requirement, compared with the same equalizers for transmission over TI channels or for time-varying channels when the transition tables are recomputed at each recursion of the BCJR algorithm and/or the VA. Using the BEM, OFDM transmission can be viewed as a dual case of SC transmission; this, however, provided a BEM resolution that is equal to the block size, where the ICI support is limited to a few neighboring subcarriers. The proposed equalizers have been evaluated based on the fact that perfect CSI is known at the receiver. To facilitate more realistic scenarios, a joint channel estimation and equalization technique has also been proposed. For the joint channel estimation and equalization, a PSAM technique has been used to acquire an initial estimate of the channel. This joint channel estimation and equalization is performed in an iterative manner. Through computer simulations, we have shown that the proposed equalizers are capable of exploiting the multipath diversity in the time domain and the Doppler diversity in the frequency domain. Finally, performing the MLSE and the MAP equalizer in the time domain or in the frequency domain allows for a complexity–diversity (performance) tradeoff.

REFERENCES

[1] T. Ericson, "Structure of optimum receiving filters in data transmission systems," *IEEE Trans. Inf. Theory*, vol. IT-17, no. 3, pp. 352–353, May 1971.

[2] C. Belfiore and J. Park, "Decision feedback equalization," *Proc. IEEE*, vol. 67, no. 8, pp. 1143–1156, Aug. 1979.

[3] N. Al-Dhahir and J. M. Cioffi, "MMSE decision-feedback equalizers: Finite length results," *IEEE Trans. Inf. Theory*, vol. 41, no. 4, pp. 961–975, Jul. 1995.

[4] G. Forney, Jr., "Maximum likelihood sequence estimation of digital sequences in the presence of intersymbol interference," *IEEE Trans. Inf. Theory*, vol. IT-18, no. 3, pp. 363–378, May 1972.

[5] I. Barhumi, G. Leus, and M. Moonen, "Time-varying FIR decision feedback equalization of doubly-selective channels," in *Proc. Globecom*, Dec. 1–5, 2003, vol. 4, pp. 2263–2268.

[6] I. Barhumi, G. Leus, and M. Moonen, "Time-varying FIR equalization of doubly selective channels," *IEEE Trans. Wireless Commun.*, vol. 4, no. 1, pp. 202–214, Jan. 2005.

[7] I. Barhumi, G. Leus, and M. Moonen, "Equalization for OFDM over doubly selective channels," *IEEE Trans. Signal Process.*, vol. 54, no. 4, pp. 1445–1458, Apr. 2006.

[8] D. K. Borah and B. D. Hart, "A robust receiver structure for time-varying frequency-flat, Rayleigh fading channels," *IEEE Trans. Commun.*, vol. 47, no. 3, pp. 360–364, Mar. 1999.

[9] D. K. Borah and B. D. Hart, "Receiver structure for time-varying frequency-selective fading channels," *IEEE J. Sel. Areas Commun.*, vol. 17, no. 11, pp. 1863–1875, Nov. 1999.

[10] G. Ungerboeck, "Adaptive maximum-likelihood receiver for carrier-modulated data-transmission systems," *IEEE Trans. Commun.*, vol. COM-22, no. 5, pp. 624–636, May 1974.

[11] A. E. El-Mahdy, "Adaptive channel estimation and equalization for rapidly mobile communication channels," *IEEE Trans. Commun.*, vol. 52, no. 7, pp. 1126–1135, Jul. 2004.

[12] L. Bahl, J. Cocke, F. Jelinek, and J. Raviv, "Optimal decoding of linear codes for minimizing symbol error rates," *IEEE Trans. Inf. Theory*, vol. IT-20, no. 2, pp. 284–287, Mar. 1974.

[13] A. Viterbi, "Error bounds for convolutional codes and an asymptotically optimum decoding algorithm," *IEEE Trans. Inf. Theory*, vol. IT-13, no. 2, pp. 260–269, Apr. 1967.

[14] G. B. Giannakis and C. Tepedelenlioglu, "Basis expansion models and diversity techniques for blind identification and equalization of time-varying channels," *Proc. IEEE*, vol. 86, no. 10, pp. 1969–1986, Oct. 1998.

[15] X. Ma and G. B. Giannakis, "Maximum-diversity transmissions over doubly selective wireless channels," *IEEE Trans. Inf. Theory*, vol. 49, no. 7, pp. 1823–1840, Jul. 2003.

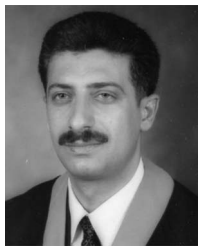
[16] M. Feder and J. Catipovitc, "Algorithms for joint channel estimation and data recovery—Application to equalization in underwater communications," *IEEE J. Ocean. Eng.*, vol. 16, no. 1, pp. 42–55, Jan. 1991.

[17] I. Barhumi, G. Leus, and M. Moonen, "Estimation and direct equalization of doubly selective channels," *EURASIP J. Appl. Signal Process.*, vol. 2006, no. 19, pp. 62 831-1–62 831-15, 2006.

[18] J. Hagenauer and P. Hoeher, "A viterbi algorithm with soft-decision outputs and its applications," in *Proc. IEEE Global Commun. Conf.*, Dallas, TX, Nov. 1989, pp. 1680–1686.

[19] H. Nguyen and B. Levy, "The expectation-maximization viterbi algorithm for blind adaptive channel equalization," *IEEE Trans. Commun.*, vol. 53, no. 10, pp. 1671–1678, Oct. 2005.

[20] F. Ling, "Matched filter-bound for time-discrete multipath Rayleigh fading channels," *IEEE Trans. Commun.*, vol. 43, no. 234, pp. 710–713, Feb.–Apr. 1995.



Imad Barhumi (M'06) received the B.Sc. degree in electrical engineering from Birzeit University, Birzeit, Palestine, in 1996, the M.Sc. degree in telecommunications from the University of Jordan, Amman, Jordan, in 1999, and the Ph.D. degree in electrical engineering from the Katholieke Universiteit Leuven (KUL), Leuven, Belgium, in 2005.

From 1999 to 2000, he was with the Department of Electrical Engineering, Birzeit University, as a Lecturer. After his Ph.D. graduation, he was a Postdoctoral Research Fellow for one year with the Department of Electrical Engineering, KUL. He is currently an Assistant Professor with the Department of Electrical Engineering, United Arab Emirates University, Al-Ain, United Arab Emirates. His research interests include signal processing for mobile and wireless communications, in particular, channel estimation and equalization of rapidly time-varying mobile wireless channels.



Marc Moonen (M'94–SM'06–F'07) received the electrical engineering (M.Sc.) and Ph.D. degrees in applied sciences from Katholieke Universiteit Leuven (KUL), Leuven, Belgium, in 1986 and 1990, respectively.

Since 2004, he has been a Full Professor with the Department of Electrical Engineering, KUL, where he is heading a research team working in the area of numerical algorithms and signal processing for digital communications, wireless communications, digital subscriber lines, and audio signal processing. He was the Editor-in-Chief for the *European Association for Signal Processing (EURASIP) Journal on Applied Signal Processing* (2003–2005) and a member of the Editorial Board of *Integration, the VLSI Journal*. He is currently a member of the Editorial Board of the *EURASIP Journal on Applied Signal Processing*, the *EURASIP Journal on Wireless Communications and Networking*, and *Signal Processing*.

Prof. Moonen has been a member of the Editorial Board of the IEEE TRANSACTIONS ON CIRCUITS AND SYSTEMS II (2002–2003) and the IEEE SIGNAL PROCESSING MAGAZINE (2003–2005). He was the recipient of the 1994 KUL Research Council Award, the 1997 Alcatel Bell (Belgium) Award (with P. Vandaele), the 2004 Alcatel Bell (Belgium) Award (with R. Cendrillon), was the 1997 "Laureate of the Belgium Royal Academy of Science," and won the Best Paper Awards from the IEEE TRANSACTIONS ON SIGNAL PROCESSING (with G. Leus) and *Elsevier Signal Processing* (with S. Doclo). He was the Chairman of the IEEE Benelux Signal Processing Chapter (1998–2002) and is currently the Past-President of EURASIP and a member of the IEEE Signal Processing Society Technical Committee on Signal Processing for Communications.